Proceedings of the 18th World Congress
The International Federation of Automatic Control
Milano (Italy) August 28 - September 2, 2011

Fault-tolerant control of an electro-hydraulic servo axes with a duplex-valve-system ⋆

Beck, Mark * **Schwung, Andreas** ** **Muenchhof, Marco** *
Isermann, Rolf *

* *TU Darmstadt, Institute of Automatic Control, Laboratory for Control Systems and Process automation, 64283 Darmstadt, Germany (e-mail: {mbeck}, {mmuenchhof}, {risermann}@iat.tu-darmstadt.de).*
** *TU Darmstadt, Institute of Automatic Control, Laboratory for Control Theory and Robotics, 64283 Darmstadt, Germany (e-mail: aschwung@rtr.tu-darmstadt.de).*

Abstract: This paper presents fault detection, fault diagnosis, the fault-tolerant control of an electro-hydraulic servo axes with a duplex-valve-system. The fault detection is based on parity equations and is load independent. The semi-physical models allow the detection of even small faults in the hydraulic system. The fault diagnosis used at the testbed is based on fuzzy-logic. In order to tolerate a faulty hydraulic proportional valve, a duplex-valve-system built up with standard proportional valves is applied. The fault management module allows the supervision of the hydraulic servo axes and decides on the reconfiguration of the control-loop. An Internal Model Control (IMC)-tracking control structure for bumpless transfer between controllers is presented. Experimental results show the industrial applicability of the approach.

Keywords: Fault Detection, Fault Diagnosis, Fault Tolerance, Electro-hydraulic Servo Axes, Duplex-valve-system, Active Fault-Tolerant Control, Reconfiguration, Bumpless-Transfer

1. INTRODUCTION

Reliability and safety of electro-hydraulic servo axes have attracted increasing attention not only in safety-related systems like aircrafts but also in common industrial hydraulic systems (consider Münchhof et al. [2009]). The costs caused by system-downtime, repair time or liability for damages often exceed the costs of a supervision module and redundant components. Different types of redundancy concepts can be applied. In case of the duplex-valve-system (see Fig. 1) considered in this paper a dynamic redundancy concept with hot standby is developed (consider Beck [2010]), where each valve is supervised by a fault detection and isolating (FDI) module (see Blanke et al. [2006]). In faultfree operation both valves are active. The advantages of this operation mode are the avoidance of clogging of the valves and the possibility of permanent supervision of both valves. If a severe fault occurs in either of the valves and is detected by the FDI-modules, the spool of the faulty valve is moved to the neutral position. To achieve the neutral position, a passive and an active way exist. The passive way is to simply shutdown the power electronics of the electromagnets, such that the centering springs push the valve spool in the neutral position. The active way is to set the reference value of the faulty valve to zero, such that the two electromagnets push the valve spool in the neutral position. The active way is only possible, if the valve spool position control loop (see Fig. 2: minor control loop) is still operable. Otherwise only the passive way is applicable. If the valve spool is moved to the neutral position, the position controller of the faulty valve should be shut down (for detailed information see Beck et al. [2009]).

The piston position control loop represents the major control loop. This control loop has to be designed fault-tolerant, i.e. the controller performance should in case of a fault still be as close to the nominal performance as possible. Basically, two different approaches exist to achieve fault tolerance (see Patton [1997]), namely passive and active fault-tolerant control (FTC). In the first case, the controller is designed to deal with faults without the adaption of the controller parameters. Often, methods of robust control theory are used. The second approach is active fault-tolerant control where either the manipulated and measured variables are modified (fault accommodation) or the control loop is reconfigured (control reconfiguration) after the detection and diagnosis of a fault. In this paper the focus is on control reconfiguration of an electro-hydraulic servo axes with a redundant duplex-valve-system and in particular on the bumpless transfer between controllers.

The paper is organized as follows. In Section 2, the process model based fault detection with parity equations for the early detection of small faults in the electro-hydraulic servo

⋆ This work was supported by the Bundeministerium fuer Wirtschaft und Technologie (BMWi)

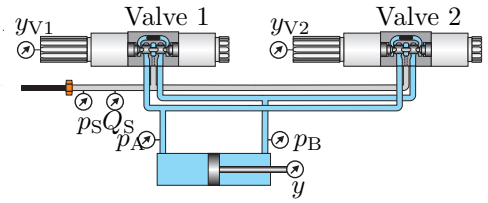

Fig. 1. Schematic assembly of the testbed with a duplex-valve-system.

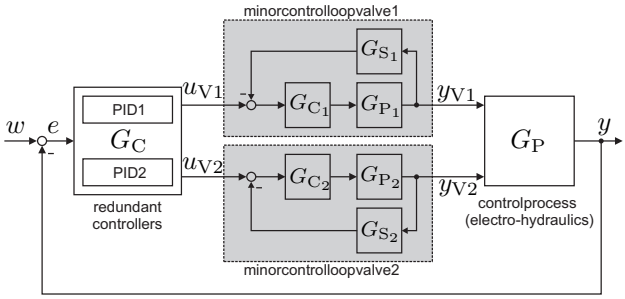

Fig. 2. Schematic assembly of the major and minor control loops.

axes is presented. The observed symptoms are evaluated by a fuzzy-logic diagnosis system. The reconfiguration of the position control loop of the servo axes with a duplex-valve-system in case of a faulty valve and also the controller design are explained in Section 3. In this section, the focus is on the IMC-based tracking control structure which allows the bumpless transfer between controllers. In Section 4, the theoretically investigated methods are applied to an existing electro-hydraulic servo axes with a duplex-valve-system. The verification at the testbed points out the industrial applicability of the approach. In Section 5, a short conclusion and an outlook is presented.

2. FAULT DETECTION AND DIAGNOSIS

Fault detection and diagnosis of the electro-hydraulic system are very important if the duplex-valve-system operates as a dynamic redundancy system. Since the spare valve is activated/deactivated depending on the system state (e.g. faultfree operation or degraded operation), the electro-hydraulic system must be supervised by a Fault Detection and Isolation (FDI) module (see Fig. 10). As shown in [Münchhof, 2006] and [Beck, 2010], parity equations (based on semi-physical models) and estimation of physical parameters (see Isermann [2006]) allow an early and reliable detection of even small faults. The subsequent fault diagnosis module (see Fig. 3) is based on a fuzzy-logic diagnosis system which allows the online diagnosis of detected faults and runs on a rapid control prototyping system (dSPACE-system) in realtime.

2.1 PROCESS MODEL BASED FAULT DETECTION

In this subsection the process model based fault detection of the 4 ports 3 way proportional valves (Manufacturer: Bosch/Rexroth, Type: 4WRE Valve) and the hydraulic cylinder is presented. Fig. 3 shows the three fault detection modules and the fault diagnosis module that allow the supervision of the electro-hydraulic system. Theoretical investigations and measurements at a testbed (see Beck [2010]) have shown that the process model based fault detection is particularly suitable for the detection of small faults in the proportional valves. Although model-based fault detection presented in [Beck et al., 2009] has been developed for hydraulic proportional valves, the methods can be applied to many other electromagnetic actuators as well.

The proportional valves used at the testbed are typical examples of mechatronic systems (see Isermann [2005]). The valve spool of the proportional valve is moved by two direct-current electromagnets. Such electromagnetic actuators contain different energy conversion mechanisms. First, the electric energy supplied to the actuator is converted into magnetic energy, which is subsequently converted into mechanical energy. The position of the valve spool is measured with a linear variable differential transformer and controlled by a minor position controller (see Fig. 2). The spool position affects the volume flow rate over the four control edges of the proportional valve. Faults can affect the electro-magnetic energy conversion as well as the magneto-mechanic energy conversion. In order to detect faults in the minor control loops of the hydraulic valves, closed-loop applicable model-based fault detection methods (consider Isermann [2006]) are implemented. Therefore, in [Beck et al., 2009], models are presented that cover both the electro-magnetic energy conversion as well as the magneto-mechanic energy conversion. Two isolating parity equations for the electromagnetic part of direct-current electromagnets and one parity equation for the magneto-mechanic part of the valve allow the detection of small faults in closed loop operation. For detailed informations about the parity equations consider Beck et al. [2009].

The overall duplex-valve-system used for building up a fault-tolerant valve-system consists of two standard hydraulic proportional valves that are mounted in parallel (see Fig. 1). Thus, the valves of the duplex-valve-system can be controlled separately. The fault detection modules presented by Beck et al. [2009] allow the supervision of the hydraulic valves. Not only the valves, but also the hydraulic cylinder should be supervised by a FDI module. For this reason model based fault detection for a hydraulic cylinder is presented in this paper. The differential cylinder (schematically shown in Fig. 1) used at the testbed is a double acting differential cylinder with a one-sided piston rod. The pressure built-up in chamber A and chamber B can be described by (see Münchhof [2006])

$$\dot{p}_A(t) = \frac{E\left(Q_A - G_{AB}\left(p_A(t) - p_B(t)\right) - A_A\dot{x}(t)\right)}{V_{0A} + A_A x(t)}, \quad (1)$$

$$\dot{p}_B(t) = \frac{E\left(Q_B + G_{AB}\left(p_A(t) - p_B(t)\right) + A_B\dot{x}(t)\right)}{V_{0B} - A_B x(t)}, \quad (2)$$

with

E:	bulk modulus,
A_A:	active piston area chamber A
A_B:	active piston area chamber B
$V_{0A,0B}$:	dead volume chamber A, B
$Q_{A,B}$:	volume flow (chamber A,B)

and

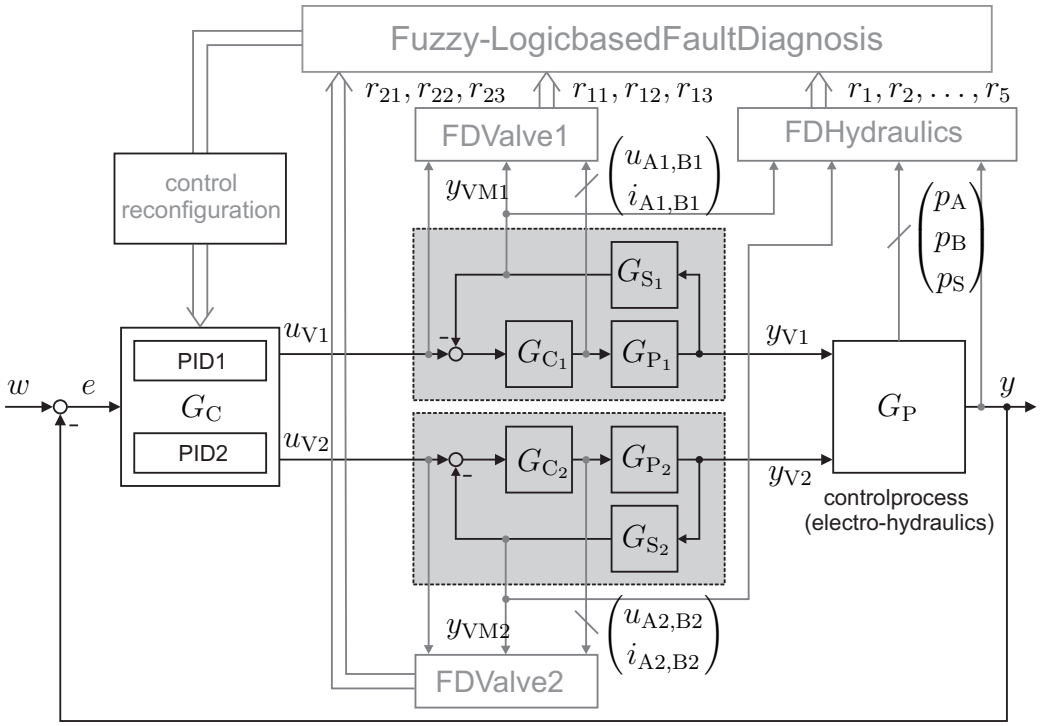

Fig. 3. Fault detection and diagnosis modules and control reconfiguration.

G_{AB} :	laminar leakage coefficient
$p_{A,B}$:	pressure in chamber A,B
p_S:	supply pressure
x:	piston position
y:	measured piston position.

In order to detect faults in the hydraulic system four residuals based on parity equations are formulated. With negligence of internal leakage ($G_{AB} = 0$) the pressure built-up can be modelled by

$$\hat{\dot{p}}_A(t) = \frac{E\left(\hat{Q}_{PA} - \hat{Q}_{AT} - A_A\dot{y}(t)\right)}{V_{0A} + A_A y(t)}, \tag{3}$$

$$\hat{\dot{p}}_B(t) = \frac{E\left(\hat{Q}_{PB} - \hat{Q}_{BT} + A_B\dot{y}(t)\right)}{V_{0B} - A_B y(t)}, \tag{4}$$

with

$$\hat{Q}_A = \hat{Q}_{PA} - \hat{Q}_{AT}, \quad \hat{Q}_B = \hat{Q}_{PB} - \hat{Q}_{BT}, \tag{5}$$

and with the modelled volume flow rates over the control edges

$$\hat{Q}_{PA} = \hat{A}_{PA}(s_0, y_{V1}, y_{V2}) \cdot \sqrt{\frac{2}{\rho}} \cdot \sqrt{p_S - p_A} \tag{6}$$

$$\hat{Q}_{AT} = \hat{A}_{AT}(s_0, y_{V1}, y_{V2}) \cdot \sqrt{\frac{2}{\rho}} \cdot \sqrt{p_A} \tag{7}$$

$$\hat{Q}_{PB} = \hat{A}_{PB}(s_0, y_{V1}, y_{V2}) \cdot \sqrt{\frac{2}{\rho}} \cdot \sqrt{p_S - p_B} \tag{8}$$

$$\hat{Q}_{BT} = \hat{A}_{BT}(s_0, y_{V1}, y_{V2}) \cdot \sqrt{\frac{2}{\rho}} \cdot \sqrt{p_B} \tag{9}$$

$\hat{A}_{PA}$:	cross section area ($P \to A$)
$\hat{A}_{AT}$:	cross section area ($A \to T$)
$\hat{A}_{PB}$:	cross section area ($P \to B$)
$\hat{A}_{BT}$:	cross section area ($B \to T$)

Due to the negligence of G_{AB} in the above parity equations, an increasing leakage becomes visible in the residuals and can be detected. The modeling of the 4 way 3 ports proportional valve and in particular the modeling of the volume flow rates over the control edges is described in [Beck, 2010], where a semi-physical model of the proportional valve is considered. The parameters of the model are obtained by measurements at the testbed and identification methods. With (3) residual r_1 can be formulated as

$$r_1 = \dot{p}_A - \hat{\dot{p}}_A. \tag{10}$$

The derivation with respect to time of the measured piston position $\dot{y}$ and the pressures, $\dot{p}_A$, $\dot{p}_B$ are each obtained by a state variable filter (SVF). The design of SVF is described in [Isermann, 1992].The pressure p_A and p_B are measured with common pressure transmitters. Analog to residual r_1 residual r_2 can be formulated with (4) as

$$r_2 = \dot{p}_B - \hat{\dot{p}}_B. \tag{11}$$

The residuals r_3 and r_4 are also based on parity equations. The velocity of the hydraulic piston, $\dot{y}$, is modelled. With rearrangement of (3), the residual r_3 follows to

$$r_3 = \dot{y} - \hat{\dot{y}}. \tag{12}$$

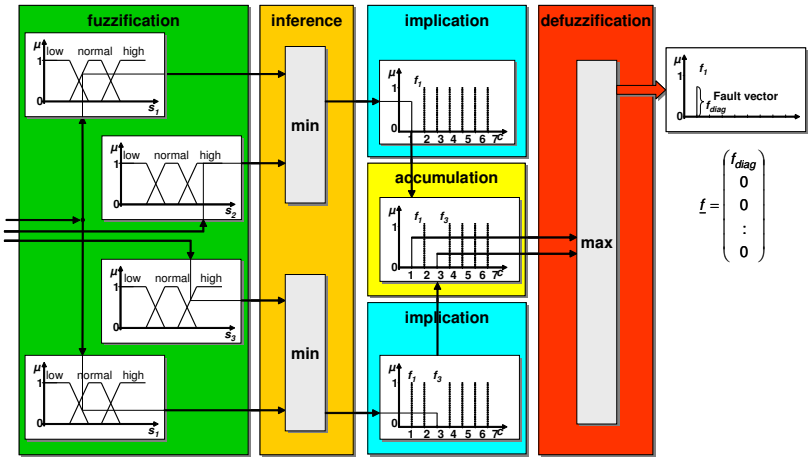

Fig. 4. Fuzzy-logic based system for fault diagnosis.

The derivation of the pressure p_{A} with respect to time $\dot{p}_{\mathrm{A}}$ is obtained by a SVF. Analog to residual r_3, residual r_4 is obtained by the rearrangement of (4). The residual r_4 follows to

$$r_4 = \dot{y} - \hat{\dot{y}}, \tag{13}$$

where the derivation of the pressure p_{B} with respect to time $\dot{p}_{\mathrm{B}}$ is again obtained by a SVF. Additionally, we monitor the operating range of the manipulated signals y_{V1} (valve 1) and y_{V2} (valve 2). If the manipulated signal is below or above of two given tresholds, the symptom is set to one, i.e., we obtain

$$r_5 = \begin{cases} 0, & \text{if } y_{\mathrm{V,min}} < y_{\mathrm{V1}} < y_{\mathrm{V,max}} \\ 1, & \text{else} \end{cases} \tag{14}$$

$$r_6 = \begin{cases} 0, & \text{if } y_{\mathrm{V,min}} < y_{\mathrm{V2}} < y_{\mathrm{V,max}} \\ 1, & \text{else} \end{cases} \tag{15}$$

Symptom r_5 and r_6 are especially suited for detecting stuck faults of the piston. In faultfree operation of the electro-hydraulic servo axes the residuals r_1, r_2, r_3 and r_4 show only small deflections caused by model uncertainty and measurement noise.

2.2 FAULT DIAGNOSIS

Both fault symptom tables 1 and 2 (Beck et al. [2009]) show a causality between the induced faults and the reaction of the residuals. The goal of fault diagnosis is to derive the existence of faults from the observed symptoms. The fault diagnosis is based on a fuzzy-logic system approach which allows to abandon the crisp separation of different fault states and uses a soft transition from one state to the other. The states are described by linguistic terms such as *reduced* or *increased*. The heuristic knowledge about the causality between symptoms and faults is implemented in the diagnostic system by means of IF-THEN rules. The overall setup of the fuzzy-based diagnosis system is illustrated in Fig. 4. For a detailed description of fuzzy-logic systems for fault diagnosis consider [Isermann, 2006].

Table 1. Fault-Symptom table of the proportional valves (Beck et al. [2009]). The residuals are defined as $r_{x1} = y_{\mathrm{Vx}} - \hat{y}_{\mathrm{Vx}}$, $r_{x2} = I_{A_x} - \hat{I}_{A_x}$ and $r_{x3} = I_{B_x} - \hat{I}_{B_x}$, where y_x is the spool position of the xth valve and I_{A_x}, I_{B_x} are the coil currents.

Fault	r_{x1}	r_{x2}	r_{x3}
Partial winding short (coil A)	+	+	o
Partial winding short (coil B)	-	o	+
Current offset ΔI_A	±	±	o
Current offset ΔI_B	±	o	±
Overheated coil A	o	-	o
Overheated coil B	o	o	-
Blocked piston valve	±	o	o
Offset position sensor	±	o	o

$x \in 1,2$	Valve 1,2
o	no deflection
+	positive deflection
-	negative deflection

Table 2. Fault-Symptom table of the hydraulic system.

Fault	r_1	r_2	r_3	r_4	r_5	r_6
faultfree	o	o	o	o	o	o
offset $\Delta p_{\mathrm{A}} \geq \pm 5\%$	±	o	±	o	o	o
offset $\Delta p_{\mathrm{B}} \geq \pm 5\%$	o	±	o	∓	o	o
leakage $G_{\mathrm{AB}} > 0$	+	-	+	+	o	o
blocking $x = const.$	o	o	o	o	+	+
sensor fault $y = const.$	-	+	-	-	+	+

o	no deflection
+	positive deflection
-	negative deflection

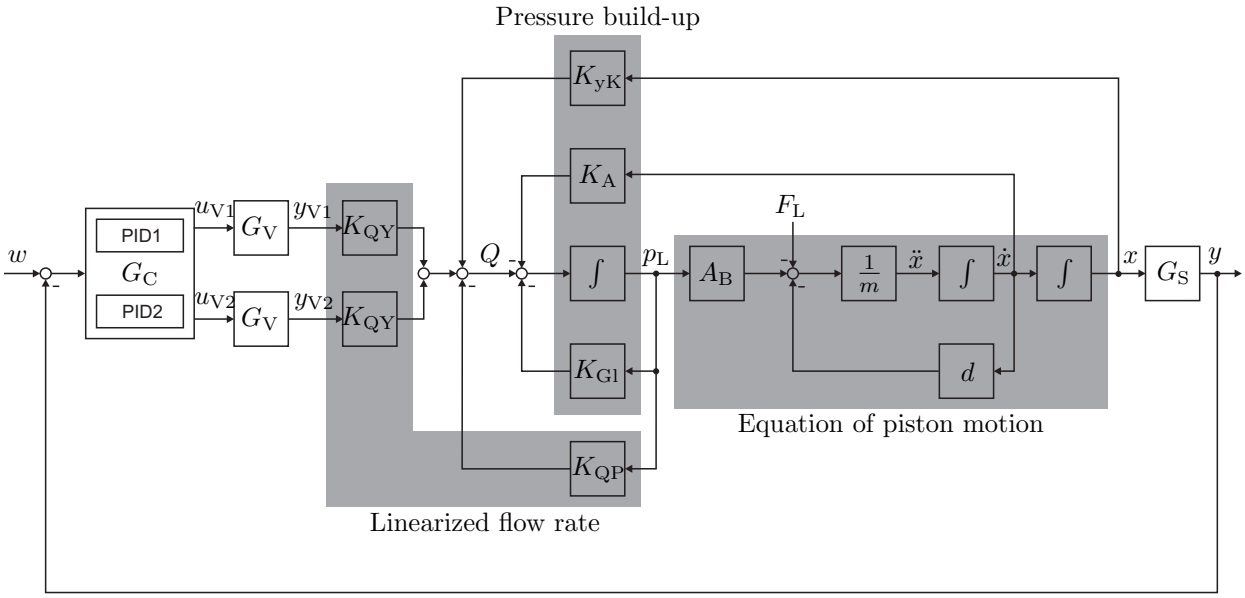

Fig. 5. Block schematics of the linearized electro-hydraulics axes with a duplex-valve-system.

3. RECONFIGURATION OF THE CONTROL LOOP

This section is divided in three subsections. In subsection 3.1 the nonlinear model of the hydraulic servo axes with a duplex-valve-system (see [Beck, 2010]) is linearized by Taylor series. The obtained linear model eases the analysis of the closed loop stability. The root locus of the faultfree hydraulic system with both valves being active is investigated. In the first part of the subsection 3.2 a robust controller is designed with the help of the linearized hydraulic model. This robust controller is used for the faultfree case (both valves active) as well as for the case of a valve failure. For these cases the Pole-Zero Map of the controlled system is studied. Based on the results of the robust controller design, a controller redesign for the faulty case is considered. Finally, in subsection 3.3 IMC-based tracking loops for bumpless transfer between controllers are presented.

3.1 Derivation of the linearized state space model

Each hydraulic valve of the duplex-valve-system is controlled by a minor control loop. These minor control loops are schematically depicted in Fig. 2. The controllers of the minor loops are proportional plus integral state controllers (Botchak [2009]). This kind of state controllers allows (with consideration of actuator saturation) the free choice of the closed-loop poles of the hydraulic valve. As minor loop controllers the proportional plus integral state controllers show a better control transfer function than standard PID controllers (see (Botchak [2009])). The four poles of the minor control loop of each valve are placed on the real axis to $p_{1,2,3,4} = -200$. Thus, the transfer function of the controlled hydraulic valves can be simplified to four PT_1 elements

$$G_V = \frac{y_{V1}}{u_1} = \frac{y_{V2}}{u_2} = \left(\frac{1}{1+0.005s}\right)^4 \tag{16}$$

The dynamics of the minor control loops are much faster than the major position control loop. Thus, a reduced state space model of the hydraulic servo axes with a duplex-valve-system is introduced. The inputs of the reduced state space model are the signals y_{V1} and y_{V2} instead of u_1 and u_2. The nonlinear model of the control process was derived by Beck [2010]. The nonlinear state space model is

$$\begin{bmatrix} \dot{x} \\ \ddot{x} \\ \dot{p}_L \end{bmatrix} = \begin{bmatrix} \dot{x} \\ -\frac{d}{m} \cdot \dot{x} + \frac{A_B}{m} \cdot p_L + \frac{1}{m} \cdot F_L \\ \frac{\alpha E}{V_A} Q_1 - \frac{E}{V_B} Q_2 \end{bmatrix} \tag{17}$$

with the abbreviations

$$Q_1 = Q_A - A_A \dot{x} - G_{AB} \cdot \frac{p_S(1-\alpha) + 2p_L}{1+\alpha} \tag{18}$$

$$Q_2 = -Q_B + A_B \dot{x} + G_{AB} \cdot \frac{p_S(1-\alpha) + 2p_L}{1+\alpha} \tag{19}$$

$$\alpha = \frac{A_A}{A_B} \tag{20}$$

$$V_A = V_{0A} + A_A \cdot x \tag{21}$$

$$V_B = V_{0B} - A_B \cdot x \tag{22}$$

This nonlinear model is linearized by Taylor series. The parameters of the linearized hydraulic model depend on the operation point of the hydraulic servo axes. The operation point can be described by

x_{op}	:	piston position in operation point
p_{Lop}	:	load pressure in operation point
y_{V1op}	:	spool position in operation point (Valve 1)
y_{V2op}	:	spool position in operation point (Valve 2)

The equation of the piston motion is

$$\ddot{x} = \frac{1}{m}\left(-F_L + A_B \cdot p_L - d \cdot \dot{x}\right) \tag{23}$$

with

m	:	piston mass
A_B	:	active area chamber B
p_L	:	load pressure
F_L	:	external load force

The resulting linearized state space model is

$$\begin{bmatrix} \dot{x} \\ \ddot{x} \\ \dot{p}_\mathrm{L} \end{bmatrix} = A \cdot \begin{bmatrix} x \\ \dot{x} \\ p_\mathrm{L} \end{bmatrix} + B \cdot \begin{bmatrix} y_{\mathrm{V}1} \\ y_{\mathrm{V}2} \end{bmatrix} + \begin{bmatrix} 0 \\ -\dfrac{1}{m} \\ 0 \end{bmatrix} \cdot [F_\mathrm{L}] \tag{24}$$

with

$$A = \begin{bmatrix} 0 & 1 & 0 \\ 0 & -\dfrac{d}{m} & \dfrac{A_\mathrm{B}}{m} \\ K_\mathrm{yK} & K_\mathrm{A} & (K_\mathrm{QP} + K_\mathrm{Gl}) \end{bmatrix} \tag{25}$$

$$B = \begin{bmatrix} 0 & 0 \\ 0 & 0 \\ K_\mathrm{QY} & K_\mathrm{QY} \end{bmatrix} \tag{26}$$

The parameters of this linearized state space model are

$$K_\mathrm{QY} = \frac{\alpha E}{V_\mathrm{A,op}} K_\mathrm{QY,A} + \frac{E}{V_\mathrm{B,op}} K_\mathrm{QY,B} \tag{27}$$

$$K_\mathrm{Gl} = \left(\frac{-\alpha}{V_\mathrm{A,op}} - \frac{1}{V_\mathrm{B,op}} \right) \frac{2EG_\mathrm{AB}}{(1+\alpha)} \tag{28}$$

$$K_\mathrm{A} = \frac{-\alpha E A_\mathrm{A}}{V_\mathrm{A,op}} - \frac{E A_\mathrm{B}}{V_\mathrm{B,op}} \tag{29}$$

$$K_\mathrm{QP} = \frac{\alpha E}{V_\mathrm{A,op}} K_\mathrm{QP,A} + \frac{E}{V_\mathrm{B,op}} K_\mathrm{QP,B} \tag{30}$$

$$K_\mathrm{yK} = -\frac{\alpha E A_\mathrm{A}}{(V_\mathrm{A,op})^2} \cdot (K_\mathrm{QY,A} \cdot x_\mathrm{op} + K_\mathrm{QP,A} \cdot p_\mathrm{Lop} - \tag{31}$$

$$A_\mathrm{A} \dot{x}_\mathrm{op} - K_\mathrm{GAB}) - \frac{E A_\mathrm{B}}{(V_\mathrm{B,op})^2} \cdot (-K_\mathrm{QY,B} \cdot x_\mathrm{op} \tag{32}$$

$$- K_\mathrm{QP,B} \cdot p_\mathrm{L,op} + A_\mathrm{B} \dot{x}_\mathrm{op} + K_\mathrm{GAB}) \tag{33}$$

with the abbreviations

$$V_\mathrm{A,op} = V_\mathrm{0A} + A_\mathrm{A} \cdot x_\mathrm{op} \tag{34}$$

$$V_\mathrm{B,op} = V_\mathrm{0B} - A_\mathrm{B} \cdot x_\mathrm{op} \tag{35}$$

$$K_\mathrm{QY,A} = C_\mathrm{PA} \cdot \sqrt{\frac{2}{\rho}} \cdot \sqrt{\frac{\alpha p_\mathrm{S} - p_\mathrm{Lop}}{1+\alpha}} \tag{36}$$

$$+ C_\mathrm{AT} \cdot \sqrt{\frac{2}{\rho}} \cdot \sqrt{\frac{p_\mathrm{S} + p_\mathrm{Lop}}{1+\alpha}} \tag{37}$$

$$K_\mathrm{QY,B} = C_\mathrm{BT} \cdot \sqrt{\frac{2}{\rho}} \cdot \sqrt{\frac{\alpha p_\mathrm{S} - p_\mathrm{Lop}}{1+\alpha}} \tag{38}$$

$$+ C_\mathrm{PB} \cdot \sqrt{\frac{2}{\rho}} \cdot \sqrt{\frac{p_\mathrm{S} + p_\mathrm{Lop}}{1+\alpha}} \tag{39}$$

$$K_\mathrm{QP,A} = \frac{1}{\sqrt{1+\alpha}} \left(\frac{-C_\mathrm{PA}(\mathrm{s}_0 + \mathrm{x}_\mathrm{op})}{2\sqrt{\alpha p_\mathrm{S} - p_\mathrm{L,op}}} \right. \tag{40}$$

$$\left. - \frac{G_\mathrm{AT}(s_0 - x_\mathrm{op})}{2\sqrt{p_\mathrm{S} + p_\mathrm{L,op}}} \right) \tag{41}$$

and

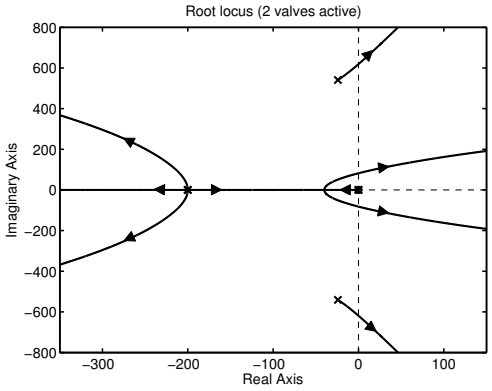

Fig. 6. Root locus of the faultfree control process with a duplex-valve-system (2 active valves).

$$K_\mathrm{QP,B} = \frac{1}{\sqrt{1+\alpha}} \left(\frac{-C_\mathrm{BT}(\mathrm{s}_0 + \mathrm{x}_\mathrm{op})}{2\sqrt{\alpha p_\mathrm{S} - p_\mathrm{L,op}}} \right. \tag{42}$$

$$\left. - \frac{G_\mathrm{PB}(s_0 - x_\mathrm{op})}{2\sqrt{p_\mathrm{S} + p_\mathrm{L,op}}} \right) \tag{43}$$

$$K_\mathrm{GAB} = G_\mathrm{AB} \frac{p_\mathrm{S}(1-\alpha) + 2p_\mathrm{L,op}}{(1+\alpha)} \tag{44}$$

The linear block schematics of the hydraulic servo axes with a duplex-valve-system is depicted in Fig. 5. In the faultfree case, both valves are active and the control loop is stabilized by a PI controller. The root locus of the control process with a duplex-valve-system in the faultfree case is depicted in Fig. 6.

3.2 Controller design and control reconfiguration

In the first part of this subsection, a robust controller is designed with the help of the linearized hydraulic model and the root locus method (see Sec. 3.1). This robust controller has fixed parameters and stabilizes the process in the faultfree case (both valves active) as well as in the case of a faulty valve. If only one valve is operable, the pressure gain and also the flow rate gain of the duplex-valve-system decreases (see [Beck, 2010]. The parameters of the robust controller must be tuned relatively conservative in order to ensure the stability of the control loop even in case of a faulty valve. Thus, the closed loop Pole-Zero map for the faultfree case as well as for the faulty case is studied. In the Pole-Zero map, see Fig. 7, the black poles and zeros represent the faultfree case. In case of a faulty valve the poles and zeros move (see Fig. 7: grey poles and zeros). In this case, the closed loop is still stable. The corresponding step responses are also depicted in Fig. 7. The transient times

$$t_\mathrm{faultfree} = 1.77 \text{ sec} - 1.66 \text{ sec} = 0.11 \text{ sec} \tag{45}$$

$$t_\mathrm{faulty} = 2.74 \text{ sec} - 1.66 \text{ sec} = 1.08 \text{ sec} \tag{46}$$

as well as the overshoots (see Fig. 7) are considerably different.

Hence, we need a control reconfiguration in order to achieve a good control performance even in case of a faulty valve. Thus, a controller G_C1 is designed to operate with both valves being active, while controller G_C2 is designed to operate with only one valve being active. These both controllers are designed with the help of the linearized

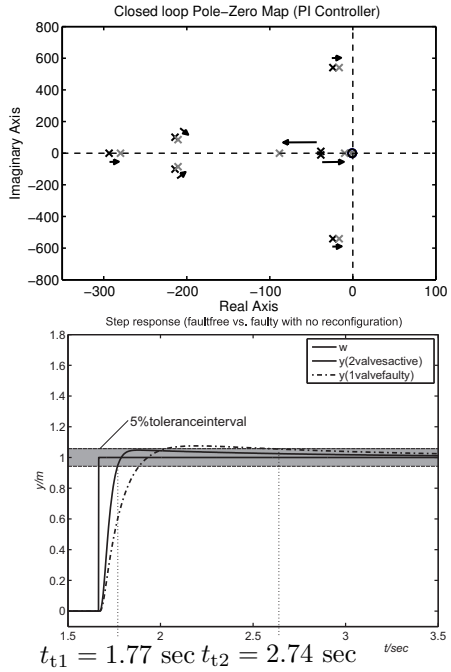

Fig. 7. Upper figure: Pole-Zero Map in the faulfree case (2 valves active, black poles) and in the faulty case (1 valve faulty, grey poles); Lower figure: step responses.

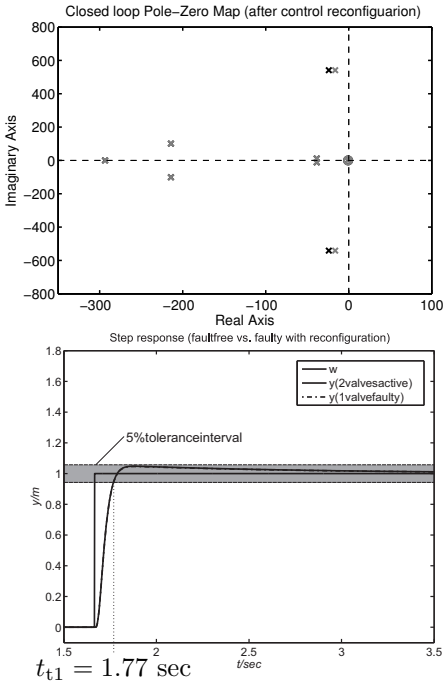

Fig. 8. Upper figure: Pole-Zero Map in the faulfree case (2 valves active, black poles) and in the faulty case (1 valve faulty after control reconfiguration, grey poles); Lower figure: step responses (nearly identical).

hydraulic model and the root locus method (see Sec. 3.1). The closed loop Pole-Zero map for the faultfree case with controller G_{C1} being active as well as for the faulty case with controller G_{C2} being active is studied. In the Pole-Zero map, see Fig. 8, the black poles and zeros represent the faultfree case, while the grey poles and zeros represent the reconfigured case. The corresponding step responses are also depicted in Fig. 8. The transient times and the overshoots are nearly identical. Thus, even in case of a faulty valve the control loop has a high control performance after control reconfiguration. The great disadvantage of the control reconfiguration is the requirement of a switching between the controllers G_{C1} and G_{C2}. This switching should provide a smooth transition of the manipulated variables. In order to guarantee this smooth transition, the bumpless transfer problem and a solution for this problem is presented in subsection 3.3.

3.3 Bumpless Transfer between controllers

In this section switching techniques for controllers are considered. A good overview of switching techniques for controllers can be found in [Schwung, 2007] and Zaccarian and Teel [2002]. Generally, hard switching and soft switching techniques are distinguished. In this paper a hard switching approach with bumpless transfer of the actuating variables is considered, which is based on tracking control (see Zaccarian and Teel [2002], Graebe and Ahlen [1996]). In order to avoid bumps to the process when switching between the output of the active controller (u_1) and the output of the inactive controller (u_2), the outputs of the controllers should be nearly the same. In industrial applications the position of the hydraulic piston is often controlled by a standard PID controller. Since the PID controller is unstable according to the bibo-(bounded input bounded output) criterion, the inactive

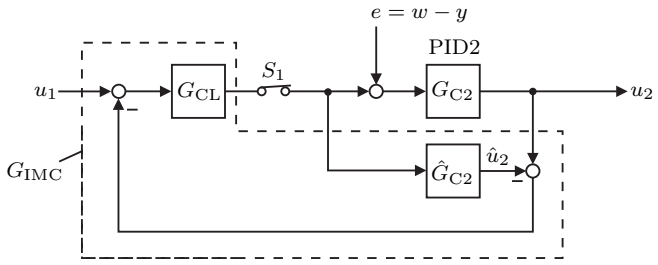

Fig. 9. IMC-based control loop for continous tracking of the inactive controller (PID2).

controller must be operated in closed loop in order to avoid drifting. The tracking control loop stabilizes the inactive controller and tracks the output of the inactive controller to the output of the active controller. In order to solve this bumpless transfer problem the tracking control structure proposed by Graebe and Ahlen [1996] and the tracking control structure based on internal model control (IMC) were investigated in [Beck, 2010]. In direct comparison the IMC based tracking control shows better performance and easier design. For detailed information about IMC consider [Garcia and Morari, 1982]. In case of the tracking control loop, the inactive controller G_{C2} represents the controlled system. The parameters of the controllers are exactly known. Thus, the internal model $\hat{G}_{C2}$ (see Fig. 9) accord with the controlled system and no model uncertainty must be considered. In this paper only the transfer between two controllers is presented. However, the approach is also valid for stabilizing and tracking of any number of inactive controllers. Fig. 9 shows the IMC structure used for stabilization and tracking of the inactive controller G_{C2}. The reference value of this control loop is the output signal u_1 of the active controller G_{C1}. Since

model and controlled system match exactly, the controller G_{CL} only acts if there exist disturbances (see Fig. 9). In case of the tracking control the main disturbance is the control derivation e of the major loop. The input-output transfer function of the tracking loop is

$$G_{u_1,u_2} = \frac{u_2}{u_1} = \frac{G_{\mathrm{CL}} G_{\mathrm{C2}}}{1 - G_{\mathrm{CL}} \hat{G}_{\mathrm{C2}} + G_{\mathrm{CL}} G_{\mathrm{C2}}}. \quad (47)$$

The disturbance transfer function G_{e,u_2} of the tracking control loop is

$$G_{e,u_2} = \frac{u_2}{e} = \frac{\left(1 - G_{\mathrm{CL}} \hat{G}_{\mathrm{C2}}\right) G_{\mathrm{C2}}}{1 - G_{\mathrm{CL}} \hat{G}_{\mathrm{C2}} + G_{\mathrm{CL}} G_{\mathrm{C2}}}. \quad (48)$$

In case of exact known controller parameters, (47) and (48) can be simplified to

$$G_{\mathrm{u_1,u_2}} = G_{\mathrm{CL}} G_{\mathrm{C2}} \quad (49)$$
$$G_{e,u_2} = \left(1 - G_{\mathrm{CL}} G_{\mathrm{C2}}\right) G_{\mathrm{C2}}. \quad (50)$$

Optimal tracking performance and best disturbance rejection is achieved if the controller G_{CL} is chosen as

$$G_{\mathrm{CL}} = G_{\mathrm{C2}}^{-1}. \quad (51)$$

However, the inverse of the controlled system G_{C2}^{-1} is often not realizable (e.g. for practical use a PID controller is expanded to a $PIDT_1$ controller and hence, the inverse does not exist). If the controller G_{C2} is minimum-phase, but has no direct feedthrough, the inverse does not exist. By expansion with a low pass G_{LP} filter of order n the controller G_{CL} can be made realizable. Thus, the controller of the IMC loop can be described by

$$G_{\mathrm{CL}} = G_{\mathrm{C2}}^{-1} G_{\mathrm{LP}} = G_{\mathrm{C2}}^{-1} \frac{K_{\mathrm{LP}}}{(1 + T_1 s)^n}. \quad (52)$$

The low pass filter G_{LP} should be designed depending on the bandwidth of the input signals. If the bandwidth of the low pass filter is high enough and if the design rules for the controller G_{CL} are considered, only small bumps occur after switching and the manipulated variable shows a smooth characteristic. If the controller G_{CL} is designed according to (52), the transfer function of the tracking loop is

$$G_{u_1,u_2} = G_{\mathrm{C2}}^{-1} G_{\mathrm{LP}} G_{\mathrm{C2}} = G_{\mathrm{LP}}. \quad (53)$$

The disturbance transfer function G_{e,u_2} is due to (52)

$$G_{e,u_2} = \left(1 - G_{\mathrm{C2}}^{-1} G_{\mathrm{LP}} G_{\mathrm{C2}}\right) G_{\mathrm{C2}} = \left(1 - G_{\mathrm{LP}}\right) G_{\mathrm{C2}}. \quad (54)$$

The resulting fault-tolerant control loop with an IMC-based tracking control loop for the inactive controller is depicted in Fig. 10. A bidirectional switching between the controller G_{C2} and G_{C1} is possible, if a tracking control loop for the active controller is also considered. For detailed information about the bidirectional switching between controllers consider [Beck et al., 2010].

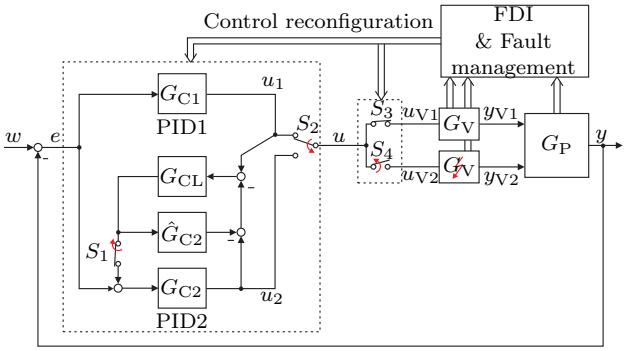

Fig. 10. Schematic assembly of the fault-tolerant control loop.

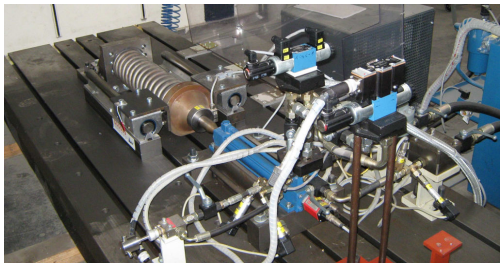

Fig. 11. Testbed with duplex-valve-system.

4. EXPERIMENTAL RESULTS

In this section the automatic reconfiguration of the control loop, as well as the bumpless transfer between the controllers G_{C1} and G_{C2} at the hydraulic testbed (see Fig. 11) are presented. The FDI modules, as well as the IMC based tracking control loop run on a Rapid-Control-Prototyping system at the testbed. A failed valve in the duplex-valve-system is simulated by a simple shut down of the valve power supply. The result of measurement series at the testbed is depicted in Fig. 12. In the first frame of Fig. 12 both valves are active and the controller G_{C1} stabilizes the control loop. This frame represents the faultfree case. At time $t = 16.8\ sec$ the power supply of the second valve is shut down. Thus, the valve spool of the faulty valve is uncontrollable. In this case, the strong centering springs immediately move the spool of the failed valve in the neutral position (see Fig. 12: $y_{\mathrm{V}} = 0$ for $t > 16.8\ sec$). After the detection and isolation of the valve fault by the FDI modules at time $t = 17.1 sec$, the Fault Management module switches over to the second controller G_{C2} (see frame II in Fig. 12). The switch over from controller G_{C1} to G_{C2} in Fig. 12 occurs during an dynamic excitation of the servo axes. This represents the worst case for a bumpless transfer between the controllers. But even in this worst case, only small bumps in the controlled variable occur (see frame III in Fig. 12). If the switch over is perfomed without a dynamic excitation of the servo axes, no bumps at all occur.

5. CONCLUSION AND OUTLOOK

In this paper realtime capable fault detection modules based on process model-based and signal-based fault detection methods are considered. The fuzzy-logic diagnosis system presented in this paper is well-established for the online diagnosis of faults. Moreover, the reconfiguration

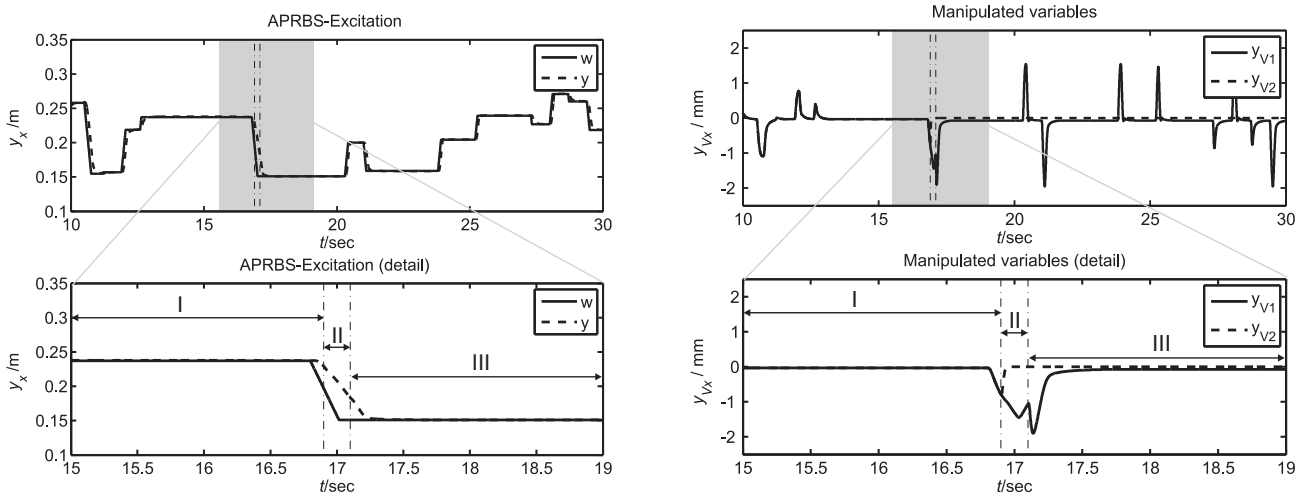

Fig. 12. Control reconfiguration in case of a valve failure. Frame I: PID1 active, 2 valves active (faultfree case). Frame II: PID1 active, valve 1 faultfree, valve 2 faulty. Frame III: Faulty valve detected and isolated by FDI-modules. Bumpless transfer to PID2, valve 1 active, valve 2 inactive (reconfigured case).

of the control loop in case of a valve fault is presented. In faultfree operation the output of the inactive controller tracks to the output of the active controller. After the detection and isolation of a faulty valve in the duplex-valve-system an automatic reconfiguration of the control loop is initiated by the Fault Management module. The bumpless transfer between the output of the active controler and the output of the inactive controller is assured by an IMC based tracking control loop for the inactive controller. The methods for fault detection, diagnosis and fault-tolerant control of a duplex actuator system presented in this paper were validated on a electrohydraulic servo axes testbed. The methods are also applicable for other fault-tolerant controlled duplex systems.

ACKNOWLEDGEMENTS

The researches were grant-aided by the *Arbeitsgemeinschaft industrieller Forschungsvereinigungen Otto von Guericke e.V.* (AiF) from budgetary resources of the German *Bundesministerium fuer Wirtschaft und Technologie* (BMWi). The closing report of the AiF project 14990N is available at the *Deutsche Forschungsgesellschaft fuer Automatisierung und Mikroelektronik e.V.* (DFAM).

REFERENCES

M. Beck. Fehlertoleranzstrategien für mechatronische Systeme. Technical report, Arbeitsgemeinschaft industrieller Forschungsvereinigungen "Otto von Guericke" e.V. (BMWi), Frankfurt, Germany, 2010.

M. Beck, M. Münchhof, and R. Isermann. Model-based fault detection and diagnosis for electromagnetic valve drives. In *Proceedings of the Dynamic System and Control Conference*, Hollywood, C.A., 2009.

M. Beck, M. Münchhof, and R. Isermann. Fehlertolerante elektrohydraulische Servoachse mit Duplex-Ventilsystem. In *Tagungsband Automation 2010*, Baden-Baden, Germany, 2010.

M. Blanke, M. Kinnaert, and J. Lunze. *Diagnosis and Fault-Tolerant Control*. Springer, Berlin, 2006.

I. Botchak. Entwicklung einer modellbasierten Positionsregelung fuer ein hydraulisches 4/3 Proportionalwegeventil. Master's thesis, Technische Universität Darmstadt, Fachgebiet Elektro- und Informationstechnik, 2009.

C.E. Garcia and M. Morari. Internal Model Control: 1. a Unifying Review and Some New Results. *Ind. Eng. Chem. Process Des. Dev.*, 21:308–323, 1982.

S.F. Graebe and A.L.B. Ahlen. Dynamic transfer among alternative controllers and its relation to antiwindup controller design. *IEEE Transactions on Control Systems Technology*, 4(1):92–99, 1996.

R. Isermann. *Mechatronic systems – fundamentals*. Springer, London, 2005.

R. Isermann. *Fault-diagnosis systems – An introduction from fault detection to fault tolerance*. Springer, Heidelberg, Berlin, 2006.

R. Isermann. *Identifikation dynamischer Systeme*, volume 2. Springer, Berlin, 1992.

M. Münchhof. *Model-Based Fault Detection for a Hydraulic Servo Axis*. PhD thesis, TU Darmstadt, Fachbereich Elektrotechnik und Informationstechnik, Darmstadt, 2006.

M. Münchhof, M. Beck, and R. Isermann. Fault diagnosis and fault tolerance of drive systems. In *Proceedings of the European Control Conference*, Budapest, Hungary, 2009.

R.J. Patton. Fault-tolerant control: the 1997 situation. In *Prepr. IFAC Symposium on Fault Detection, Supervision and Safety for Technical Processes (SAFEPROCESS)*, volume 2, pages 1033–1055, Hull, United Kingdom, August 1997. Pergamon Press.

A. Schwung. Aktive Schwingungsbeeinflussung eines zeitvarianten Systems. Master's thesis, Technische Universität Darmstadt, Fachgebiet Mechatronik im Maschinenbau, 2007.

L. Zaccarian and A.R. Teel. A common framework for anti-windup, bumpless transfer and reliable designs. *Automatica*, 38(10):1735–1744, 2002.